Preprints of the 3rd IFAC Conference on Advances in Proportional-Integral-Derivative Control, Ghent, Belgium, May 9-11, 2018

WeAT1.5

Comparing Classical and Fractional Order Control Strategies of a Cardiovascular Circulatory System Simulator

José Emilio Traver[1], Inés Tejado[1], Javier Prieto-Arranz[2], Blas M. Vinagre[1]

[1] *Industrial Engineering School, University of Extremadura, 06006 Badajoz, Spain. (email: jetraverb;itejbal;bvinagre@unex.es)*
[2] *School of Industrial Engineering, University of Castilla-La Mancha, 13071 Ciudad Real, Spain. (email: Javier.PrietoArranz@uclm.es)*

Abstract: This paper compares two strategies, namely, feedback linearization (FBL) and classical proportional-integral-derivative (PID) controller, as well as their fractional versions, for the control of a simulator of the human cardiovascular circulatory system (CVS) in the Matlab/Simulink environment. The simulator is based on a hydraulic model of the system, realizable in practice, in which muscular contraction of the left ventricle is modelled by a pump with piston (tank of variable volume depending on the position of the piston), so that a control strategy is needed to control the velocity of the piston in order to emulate the behaviour of the heart. Simulations are given to demonstrate, on the one hand, that all strategies have good tracking and hemodynamic performance and, on the other, that dysfunctions in the CVS can be emulated applying an appropriate control strategy that allows tracking the desired reference waveform. The final objective of this work is the construction of an experimental platform based on this simulator to test swimming robots of small dimensions that allows to emulate the conditions in which these robots would navigate in the human circulatory system.

Keywords: Cardiovascular system, simulator, Simulink, control, fractional, microrobot.

1. INTRODUCTION

Cardiovascular diseases are the first cause of death in the world (World Health Organization (2018)). This fact exposes the severe of the situation and the need to research and develop tools that allow to evaluate and enhance its treatment. They are numerous and popular the attempts, from both the medical and the engineering community, to develop models and simulators, on the one hand, to design, evaluate and improve the working operation of ventricular assist devices and cardiac prostheses (Dasi et al. (2009)), and, on the other, to learn and evaluate about catheterization tools.

Despite the cardiovascular system (CVS) is complex, a huge amount of information can be found in the literature about its modelling (see e.g. Simaan (2009); Liu et al. (2006); Gwak et al. (2015); Yu et al. (1998)). However, there is a lack of information about how to model the arteriosclerosis disease, and especially the occlusion of arteries (stenosis) due to their thickening. This is motivated mainly for three reasons: 1) current methods, i.e., stabilization devices (stents) or bypass surgery, are focused on decreasing or removing the local pain of disease, but not removing it completely and its origin factor; 2) recent studies support greater efficacy of pharmaceutical treatments compared to invasive treatment techniques, in addition to offering a systemic treatment (Nichols et al. (2011)); and

3) the absence of devices capable of treating the disease systemically. Nevertheless, the technological advances of the last decade in the field of nano and microrobotics open up a hope of application in this branch of medicine.

In this context, this paper collects the theoretical principles that govern the dynamics of the CVS so as to develop a hydraulic simulator of this system that allows to build a experimental platform to test swimming robots of small dimensions, i.e., to emulate the conditions in which these robots would navigate in the human circulatory system. As will be shown, this simulator is based on a hydraulic model of the system, realizable in practice, in which muscular contraction of the left ventricle is modelled by a pump with piston (tank of variable volume depending on the position of the piston), so that a control strategy is need to control the velocity of the piston in order to emulate the behaviour of the heart and, consequently, obtain normal conditions of a cardiac cycle. For that purpose, both the integer and the fractional versions of two different control alternatives are compared: feedback linearization (FBL) and proportional-integral-derivative (PID) controller. Simulations are given to demonstrate, on the one hand, that all strategies have good tracking and hemodynamic performance and, on the other, that dysfunctions in the CVS can be emulated applying an appropriate control strategy that allows tracking the desired reference waveform.

The remainder of the paper is organized as follows. The functioning of the CVS is briefly explained in Section 2. Section 3 describes the simulator developed for the CVS

based on an equivalent hydraulic model. Section 4 is devoted to the control of the hydraulic model to emulate the contraction of the left ventricle. Finally, conclusions and future works are drawn in Section 5.

2. DESCRIPTION OF THE CARDIOVASCULAR SYSTEM

In order to model the CVS, this section presents a brief review of the working principle of human heart and the importance of its distribution network, as well as its hemodynamics.

In simple terms, the CVS can be understood as a distribution network (blood vessels) that supplies fluid (blood) to human body through a pump (heart).

The heart, which has the function of generating the necessary gradient of pressure to pump blood through the set of blood vessels that run through the cells of the human body, is formed by a double chamber atria-ventricle, where the atria is as pre-loaded chamber and the ventricle is, strictly speaking, the pump. The ability of the heart to generate the necessary pressure gradient lies in its ability to contract and the succession of electrical and mechanical phenomena that occur during a heartbeat, known as the cardiac cycle (Martini et al. (2015)).

The cardiac cycle is divided into two stages clearly differentiated that occur alternately: diastole (dilation period) and systole (contraction period). The change of pressure and volume that occur in the left atria and ventricle during each stage is illustrated in Fig. 1. As can be observed, the dynamics is not preserved throughout all the circulatory system, due to its diversity in morphologies, sizes and compositions. Therefore, the opposition to blood flow is also variable. Vascular resistance, understood as the friction between blood and vessel walls, depends mainly on two factors: the length and diameter of the vessel. This resistance is lower in the vascular zones (capillaries) because their total section is higher than the areas adjacent to the heart (arteries and veins).
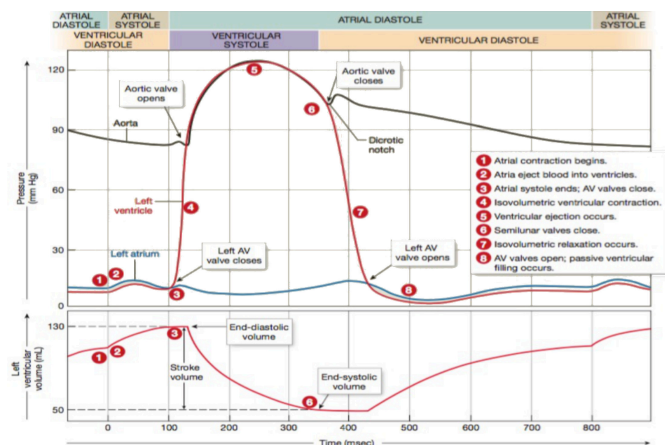

Fig. 1. Pressure and volume relationships of left atria and ventricle in the cardiac cycle. Major features of the cardiac cycle are shown for a heart rate of 75 beats per minute (bpm). Image extracted from Martini et al. (2015).

Regarding the carotid pressure, it presents slight differences in comparison with that illustrated in Fig. 1: 1) there is a time lag with respect to the systolic pressure; 2) the pressure undergoes a slight increase as a result of the reflected pressure waves; and 3) the dicrotic wave intensifies. In what the carotid flow is concerned, different behaviors can occur depending on the physiological conditions. However, its main behavior is characterized by a positive flow in a shorter period of time, followed by a negative flow caused by the closure of the aortic valve, which may even produce a second blood impulse during the ventricular diastole caused by the recoil of the blood in the descending aorta.

The repercussions of arteriosclerosis on the cardiovascular behavior are mainly two: the loss of elasticity of artery walls and artery narrowing (stenosis). The former produces an increase in the maximum pressures reached (Nichols et al. (2011)), as well as the modification of the dicrotic notch wave since the reflection of the waves occurs more quickly. On the other hand, stenosis reduces the blood flow.

3. SIMULATOR OF THE CARDIOVASCULAR SYSTEM

This section describes the simulator developed for the CVS. Firstly, an electrical model is presented. Then, considering equivalencies between domains, a hydraulic model of the CVS, realizable in practice, is presented. The latter, unlike the previous one, requires a control strategy to emulate the contraction of the left ventricle. It is important to remark that the electrical model of the CVS is given only to understand the hydraulic model, which will be the one used in simulations. The whole description of the simulator can be found in Traver et al. (2017).

3.1 Electrical model

The electrical model equivalent to the CVS is based on the Windkessel model proposed in Westerhof et al. (2009) and the corrections suggested in Yu et al. (1998). It is shown on the left part (orange shading) in Fig. 2 (Simaan (2009)). In this model, the systemic and pulmonary circulation are reduced to a total peripheral resistance (denoted as R_s), that considers the opposition to blood flow of all the arteries and veins, and a capacitance that represents the elasticity of vessels (C_s). The resistance R_c symbolises the noticeable morphology of the aortic arch, whereas L represents the inertial forces that are experimented by the blood flow due to its pulsatile nature. Likewise, heart's dynamics is solely reduced to the left side and the contraction capacity of the left ventricle (it is assumed that the right ventricle and pulmonary circulation are healthy and normal and, as a result, their effect can be neglected). The behaviour of the left ventricle is then modelled by means of a time-varying capacitance ($C(t)$) according to Frank-Starling's law (see e.g. Simaan (2009); Stergiopulos et al. (1996)), while the left atria is interpreted as a passive element of accumulation. Furthermore, valves are considered as non ideal diodes. The elasticity of the aortic valve is characterised by a capacitance (C_A), which
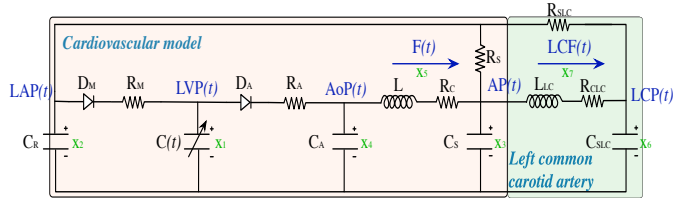
Fig. 2. Electrical model equivalent to the CVS (orange shading on the left) extended to left common carotid artery (green shading on the right).

describes the dicrotic notch wave. The cyclic nature of the CVS is achieved with a feedback in the circuit.

This model is extended to the left common carotid artery in accordance with Yu et al. (1998); Simaan (2009) (see green shading on the right in Fig. 2). The choice of this kind of artery is motivated by its high recurrence of atheroma plates Nichols et al. (2011).

It should be said that the whole model has been defined based on the anatomic structure of the circulatory system and criteria used in Westerhof et al. (2009) to develop the Windkessel model of four elements. Therefore, the resistance R_{CLC} represents the friction of flow and the bifurcation of the artery, R_{SLC} is the resistance of the blood return, L_{LC} is the inertial force due to mainly the aorta's blood flow, and the capacitance C_{SLC} is the elasticity of artery.

The differential equations that describe the dynamics of the whole system are obtained choosing the variables listed in Table 1, and applying Kirchhoff's laws to the electric circuit, except for the state x_1, which depends on the diodes and the capacitance $C(t)$, as will be shown next.

The differentiation of state x_1 results in

$$\dot{x}_1 = \frac{1}{C(t)} \left(-\dot{C}(t)x_1 + \frac{1}{R_M}r(x_2 - x_1) - \frac{1}{R_A}r(x_1 - x_4) \right) \quad (1)$$

where the function r is derived from diodes operation as

$$r(\xi) = \begin{cases} \xi, & \text{if } \xi \geq 0 \\ 0, & \text{if } \xi < 0 \end{cases} \quad (2)$$

while $C(t)$ is defined as the inverse of the elastance $E(t)$ (Simaan (2009)), i.e.,

$$E(t) = \frac{LVP(t)}{LVV(t) - V_0}, \quad (3)$$

where $LVP(t)$ and $LVV(t)$ are the pressure and volume of the left ventricle (the latter depends on the integration of the currents that flow through the diodes D_M and D_A), respectively, and V_0 is a reference volume (the theoretical volume in the ventricle at zero pressure). Further details

Table 1. Variables of the CVS model.

Variables	Name	Physiological meaning (unit)
$x_1(t)$	LVP(t)	Left ventricle pressure (mmHg)
$x_2(t)$	LAP(t)	Left atrial pressure (mmHg)
$x_3(t)$	AP(t)	Arterial pressure (mmHg)
$x_4(t)$	AoP(t)	Aortic pressure (mmHg)
$x_5(t)$	F(t)	Total blood flow (ml/s)
$x_6(t)$	LCP(t)	Left common carotid pressure (mmHg)
$x_7(t)$	LCF(t)	Blood flow of left common carotid (ml/s)

about the description used in this work for E(t) can be found in Stergiopulos et al. (1996) or in our previous work Traver et al. (2017).

The derivatives of the rest of states are obtained by applying directly Kirchhoff's laws:

$$\dot{x}_2 = \frac{1}{C_R} \left(-\left(\frac{1}{R_S} + \frac{1}{R_{SLC}} \right) x_2 + \right. \quad (4)$$
$$\left. \frac{1}{R_S}x_3 + \frac{1}{R_{SLC}}x_6 - \frac{1}{R_M}r(x_2 - x_1) \right)$$

$$\dot{x}_3 = \frac{1}{C_S} \left(\frac{1}{R_S}x_2 - \frac{1}{R_S}x_3 + x_5 - x_7 \right) \quad (5)$$

$$\dot{x}_4 = \frac{1}{C_A} \left(-x_5 + \frac{1}{R_A}r(x_1 - x_4) \right) \quad (6)$$

$$\dot{x}_5 = \frac{1}{L} \left(-x_3 + x_4 - R_C x_5 \right) \quad (7)$$

$$\dot{x}_6 = \frac{1}{C_{SLC}} \left(\frac{1}{R_{SLC}}x_2 - \frac{1}{R_{SLC}}x_6 + x_7 \right) \quad (8)$$

$$\dot{x}_7 = \frac{1}{L_{LC}} \left(x_3 - x_6 - R_{LC} x_7 \right) \quad (9)$$

The set of equations (1) and (4)–(9) defines an autonomous switched time-varying system over different phases within the cardiac cycle. Moreover, it has a strongly non linear cyclic nature because of the terms $\dot{C}(t)$ and $1/C(t)$ are strongly non-linearity. That ensures a continuous dynamics.

3.2 Hydraulic model

With the purpose to obtain a physically realizable hydraulic model of the CVS which will allow testing swimming robots of small dimensions, the following set of equivalencies between the electric and hydraulic domains, among other considerations, was defined (Chaturvedi (2009)): electric resistors, capacitances and inductances are replaced by hydraulic resistors (denoted as R_{Hi}, where the subscript i refers to the name used in the electric model), tanks with constant sections ($C_{Hi} = \frac{A}{\rho g}$, where A is the tank section, ρ is the density of fluid and g, the gravity) and long pipes ($L_{Hi} = \frac{l\rho}{A}$, where l is the length of the pipe), respectively. The diodes are changed by one-way valves. The hydraulic model of the CVS is illustrated in Fig. 3 and all their parameters are given in Table 2.

Regarding muscular contraction of the left ventricle, in the hydraulic model $C(t)$ is modelled by a pump with piston (tank of variable volume depending on the position of the piston), as shown in Fig. 4, in such a way that a control
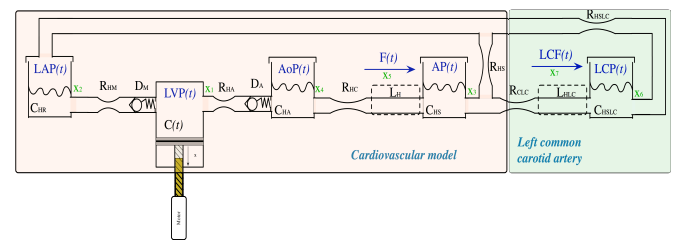

Fig. 3. Hydraulic model of the CVS.

Table 2. Parameters of the CVS model. Taken from Simaan (2009); Yu et al. (1998).

Parameter	Value	Physiological meaning (unit)
	Resistors	
R_{HS}	133.32 (MPa/(m^3/s))	Total peripheral resistance
R_{HSLC}	133.32 (MPa/(m^3/s))	Left common carotid peripheral resistance
R_{HM}	0.67 (MPa/(m^3/s))	Mitral valve resistance
R_{HA}	0.13 (MPa/(m^3/s))	Aortic valve resistance
R_{HC}	5.30 (MPa/(m^3/s))	Characteristic resistance
R_{HCLS}	26.67 (MPa/(m^3/s))	Left common carotid resistance
	Capacitances	
C_{HR}	$6.933 \cdot 10^{-2}$ (m^3/MPa)	Left atrial compliance
C_{HS}	$6 \cdot 10^{-4}$ (m^3/MPa)	Systemic compliance
C_{HA}	$9.97 \cdot 10^{-3}$ (m^3/MPa)	Aortic compliance
C_{HLC}	$6.75 \cdot 10^{-4}$ (m^3/MPa)	Left common carotid
	Inductances	
L_{HS}	$6.66 \cdot 10^{-2}$ (MPa/(m^3/s^2))	Inertance of blood in aorta
L_{HSLC}	3.99 (MPa/(m^3/s^2))	Inertance of blood in left common carotid
	Left ventricle	
E_{max}	266.64 (MPa/m^3)	Maximum volume in diastole
E_{mix}	0.79 MPa/m^3)	Minimum volume in diastole
V_0	10 (ml)	Reference volume at zero pressure
HR	75 (bpm)	Heart rate

strategy is required to emulate the behaviour of the heart (Gwak et al. (2015)). Thus, the derivative of state x_1 in this case can be expressed as:

$$\dot{x}_1 = \frac{1}{C_p}(Q_i - Q_o - A_p \nu), \qquad (10)$$

where C_p is the capacitance of piston, Q_i and Q_o are the in and out flow, respectively, A_p is the sectional area of piston, and $\nu = \dot{x}_p$ is the displacement speed of the piston (this parameter modifies the pressure of the piston chamber). Equation (10) can be also written as:

$$\dot{x}_1 = \frac{1}{C_p}\left(\frac{1}{R_{HM}}r(x_2 - x_1) - \frac{1}{R_{HA}}r(x_1 - x_4)\right) \quad (11)$$
$$- \frac{A_p}{C_p}\nu$$

The other state equations describing the hydraulic model of the CVS remain inalterable. In contrast to the electric model, now the system has non autonomous nature. Therefore, as commented, it is needed to apply a control strategy to the displacement speed of the piston in order to emulate the contraction of the left ventricle according to Frank-Starling's law.

4. CONTROL

In this section, two strategies will be compared to obtain normal conditions of a cardiac cycle with the CVS simulator, i.e., FBL and PID. In both cases, fractional dynamics will be introduced into the controller substituting the derivative by the fractional order operator.

The control scheme used for all strategies is illustrated in Fig. 5. It is important to remark that the reference
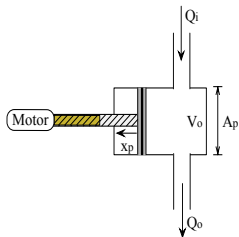
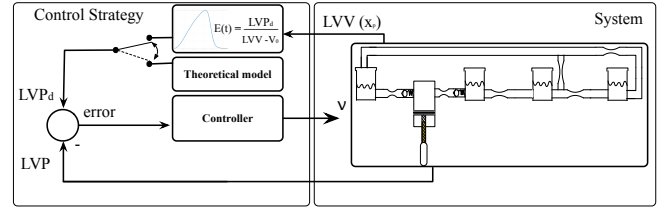Fig. 4. Hydraulic equivalence of left ventricle (pump with piston).

Fig. 5. Block diagram for the control of the CVS simulator.

LVP_d is obtained from its relation with the elastance E(t), i.e., equation (3), once the heart rate and the parameter V_0 have been set and knowing LVV(t) from the piston position. Thus, it depends on the controller applied.

4.1 Feedback Linearization Controller

The main idea of this approach is to algebraically transform a non linear system dynamics into a (fully or partly) linear one so that linear control techniques can be applied (see e.g. Slotine and Li (1991)).

Then, to linearise state variable x_1, i.e., equation (11), it is possible to take the system input ν as follows:

$$\nu = -\frac{C_p}{A_p}\left(u - \frac{1}{C_p}\left(\frac{r(x_2 - x_1)}{R_{HM}} - \frac{r(x_1 - x_4)}{R_{HA}}\right)\right), \quad (12)$$

This allows to consider a linear relation between the system output ($y = x_1$) and variable u, being u the equivalent input of the linearised dynamics, and which is considered of relative order one due to the fact that an integration between the output and the equivalent input, i.e., $\dot{y} = u$, is obtained. Taking into account this linear relation, the control law to be designed is:

$$u = \dot{y}_d - \dot{y} + \lambda(y_d - y) = \dot{e} + \lambda e, \qquad (13)$$

where y_d is the desired output, e is the error, defined as $e = y_d - y_1$, and $1/\lambda$ is the time constant of the error.

Hence, substituting (13) in (12) the following expression is obtained:

$$\nu = -\frac{C_p}{A_p}\left(\dot{e} - \frac{1}{C_p}\left(\frac{r(x_2 - x_1)}{R_{HM}} - \frac{r(x_1 - x_4)}{R_{HA}}\right) + \lambda e\right), \quad (14)$$

which allows to follow the reference in accordance with the control law established.

For this strategy, fractional dynamics is introduced by doing

$$u = D^\alpha e + \lambda e, \qquad (15)$$

where D is the fractional operator, and $\alpha \in \mathbb{R}^+$ the differentiation order. This controller will be referred henceforth to as FBL+FD.

4.2 PID Controller

A PID controller proposed in Gwak et al. (2015) is used with gains: $k_p = 0.5$, $k_i = 0.6$, and $k_d = 0.003$. It is applied directly over the controlled variable x_1.

In order to compare with the previous PID controller and the PD control law used in FBL, in this case fractional dynamics is introduced by using a three-parameter fractional controller, namely, a fractional proportional-derivative (FPD) controller.

Table 3. Controller parameters.

Strategy	λ or k_p	k_i	k_d	α
FBL	40	–	–	–
FBL+FD	40	–	–	0.2
PID	0.5	0.6	0.003	–
FPD	0.5	–	0.6	0.2

5. SIMULATIONS

This section presents the simulation results obtained when applying the control strategies described in Section 4 to the CVS simulator.

Taking in mind the final objective of the simulator, i.e., the construction of an experimental platform to test swimming robots of small dimensions so as to emulate the conditions in which these robots would navigate in the human circulatory system, the following considerations were established:

- In what the simulator is concerned, the pipes that connect the different tanks and valves were considered with a diameter of 2 inches (enough diameter to ensure free movement of the swimming robots). Likewise, the dimensions of the deposits, their section and the initial value of the fluid, are obtained from the equivalences indicated above and the values given in Table 2.
- In order to achieve microscopic phenomena produced by the interaction of microrobots with cardiovascular hemodynamics at macroscopic level, the fluid considered was 30 W oil, whose viscosity is 109.408 cSt and density 852.5 kg/m^3 at 35°. Theses properties allow to emulate the desired conditions.
- Fractional derivatives were approximated by Oustaloup method with four poles and four zeros in the frequency range $[0.01, 100]$ rad/s.
- In order to avoid chattering, the controlled variable was filtered before applying the control strategy by the low-pass filter

$$F(s) = \frac{100}{s + 100}. \tag{16}$$

- For comparison purposes, the following hemodynamic parameters will be measured in the waveforms obtained: systolic and diastolic pressure, mean aortic pressure (MAP), cardiac ouput (CO), stroke volume (SV), systolic and diastolic pressure of left ventricle (LVP), maximum and minimum volume of left ventricle (LVV), and systolic and diastolic pressure of the atrial (LAP).
- The controller parameters used for simulations are given in Table 3.

The waveforms of the hemodynamics for a healthy adult with 75 beat per minute obtained when applying the four strategies are illustrated in Fig. 6, whereas the indices measured are given in Table 4. From these results, it can be stated that all strategies, even proportional control law in FBL (i.e., $u = \lambda e$), provide good enough tracking and hemodynamic performance. So, a fractional order $\alpha = 0.2$ is chosen for comparison purposes. For all cases, the hemodynamic parameters are coherent with real hemodynamics (see e.g. Martini et al. (2015); LiDCO Ltd. (2017); Lifesciences (2017); Priebe and Skarvan (1995)).

The results obtained by replacing the reference waveform LVP$_d$ by a system-independent one (i.e., that given by the electric model of the CVS, theoretical model in Fig. 5), are plotted in Fig. 7 for integer order controllers, and in Fig. 8 for fractional order ones. As can be observed, the tracking performance is better when using fractional derivatives.

6. CONCLUSION AND FURTHER WORK

This paper has compared feedback linearization (FBL) and proportional-integral-derivative (PID) controllers, of integer and fractional order, for the control of a simulator of the human cardiovascular circulatory system (CVS) in the Matlab/Simulink environment. The simulator was based on a hydraulic model of the system, realizable in practice, which emulates the behavior of the CVS and has non autonomous character. More precisely, muscular contraction of the left ventricle was modelled by a pump with piston (tank of variable volume depending on the position of the piston), so that a control strategy was needed to control the velocity of the piston in order to emulate the behaviour of the heart. Simulations were given to demonstrate that:

(1) The control strategy applied shapes the resulting reference waveform (LVP$_d$) when using system-dependent reference generation. This can be used to emulate pathologic behavior.
(2) All strategies have good tracking and hemodynamic performance.
(3) FBL has high sensitivity to its parameter λ but low sensitivity to fractional order α. Even for $\alpha = 0$ (pure proportional control law), the results do not show large differences.
(4) When reference is independent of the controlled system, the best tracking performance is obtained with fractional controllers.

Our future works will focus on: 1) justifying the results obtained mathematically; 2) applying PID structures with two degrees of freedom; 3) shaping the resulting waveform to emulate dysfunctions in the CVS; and 4) studying the influence of the approximations of fractional operators.

REFERENCES

Chaturvedi, D.K. (2009). *Modeling and simulation of systems using MATLAB and Simulink.* CRC Press.

Dasi, L.P., Simon, H.A., Sucosky, P., and Yoganathan, A.P. (2009). Fluid mechanics of artificial heart valves. *Clinical and Experimental Pharmacology and Physiology*, 36(2), 225–237.

Gwak, K., Kim, H.D., and Kim, C. (2015). Feedback linearization control of a cardiovascular circulatory simulator. *IEEE Transactions on Control Systems Technology*, 23(5), 1970–1977.

LiDCO Ltd. (2017). Normal hemodynamic parameters. URL http://www.lidco.com/clinical/hemodynamic.php.

Lifesciences, E. (2017). Normal hemodynamic parameters and laboratory values.

Liu, Y., Allaire, P., Wu, Y., Wood, H., and Olsen, D. (2006). Construction of an artificial heart pump performance test system. *Cardiovascular Engineering*, 6(4), 151–158.

Table 4. Hemodynamic parameters and MSE when applying the proposed strategies.

| Controller	Systolic pressure (mmHg)	Diastolic pressure (mmHg)	MAP (mmHg)	CO (l/s)	SV (ml/beat)	Systolic LVP (mmHg)	Diastolic LVP (mmHg)	Max LVV (ml)	Min LVV (ml)	Systolic LAP (mmHg)	Diastolic LAP (mmHg)
FBL	107.6	71.2	83.33	5.47	73	116.2	6.42	138	65	13.12	8.74
FBL+FD	108.2	71.56	83.77	5.50	73.34	117	6.15	138.2	64.96	13.05	8.5
PID	107.8	71.28	83.45	5.48	73.1	116.2	6.16	138.3	65.21	13.03	8.56
FPD	107	71.05	83	5.44	72.57	115.1	6.58	137.9	65.33	13.04	8.79
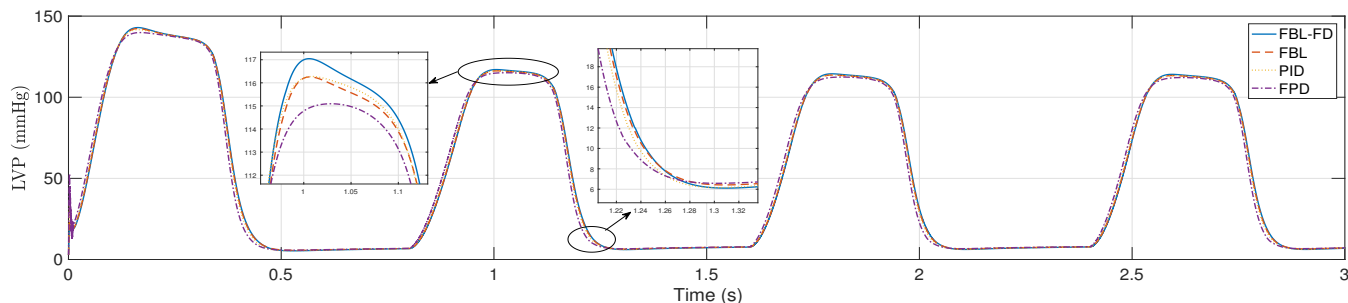
Fig. 6. Tracking performance of the LVP when applying the proposed strategies with system dependent reference.
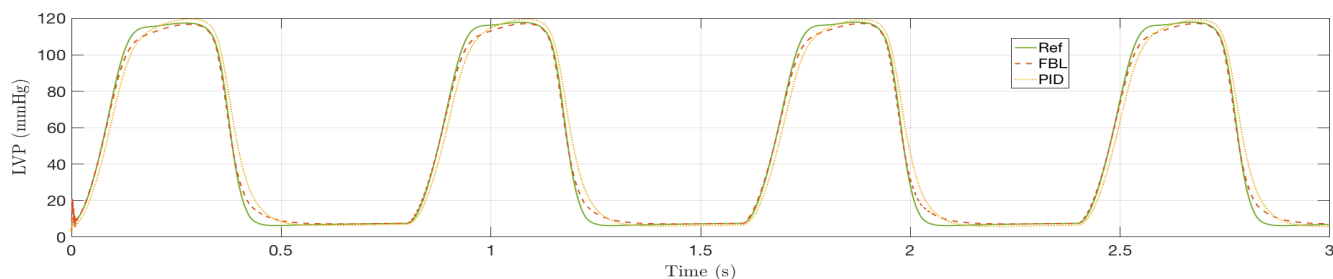

Fig. 7. Tracking performance of the LVP when applying integer order controllers with independent reference.
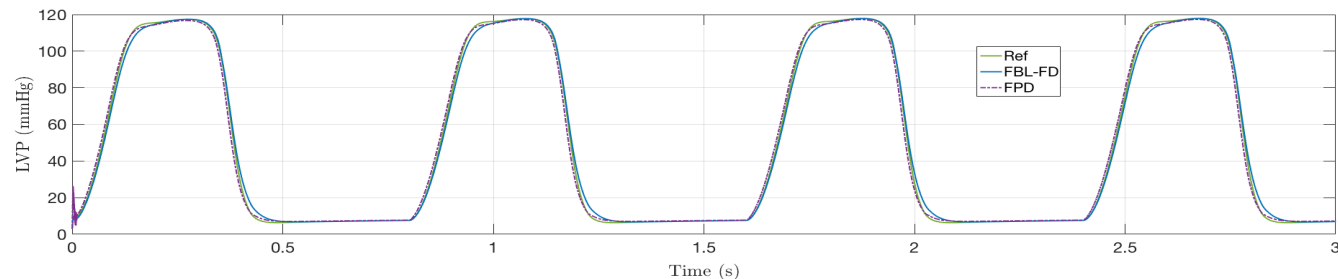

Fig. 8. Tracking performance of the LVP when applying fractional order controllers with independent reference.

Martini, F., Nath, J., and Bartholomew, E. (2015). *Fundamentals of Anatomy & Physiology*. Benjamin-Cummings Publishing Company.

Nichols, W., O'Rourke, M., and Vlachopoulos, C. (2011). *McDonald's Blood Flow in Arteries, Sixth Edition: Theoretical, Experimental and Clinical Principles*. CRC Press.

Priebe, H. and Skarvan, K. (1995). *Cardiovascular physiology*. BMJ Publishing Group.

Simaan, M.A. (2009). *Rotary Heart Assist Devices*, 1409–1422. Springer Berlin Heidelberg, Berlin, Heidelberg.

Slotine, J. and Li, W. (1991). *Applied Nonlinear Control*. Prentice-Hall International Editions. Prentice-Hall. URL https://books.google.es/books?id=HddxQgAACAAJ.

Stergiopulos, N., Meister, J., and Westerhof, N. (1996). Determinants of stroke volume and systolic and diastolic aortic pressure. *American Journal of Physiology-Heart and Circulatory Physiology*, 270(6), H2050–H2059.

Traver, J.E., Ortega, J.F., Tejado, I., Pagador, J.B., Sun, F., Pérez-Aloe, R., Vinagre, B.M., and Sánchez-Margallo, F.M. (2017). Simulador cardiovascular para ensayo de robots de navegación autónoma. In *Proceedings of XXXVIII Jornadas de Automática*, 633–640 (In Spanish).

Westerhof, N., Lankhaar, J., and Westerhof, B.E. (2009). The arterial Windkessel. *Medical & Biological Engineering & Computing*, 47(2), 131–141.

World Health Organization (2018). Cardiovascular diseases. URL http://www.who.int/cardiovascular_diseases/en/.

Yu, Y., Boston, J.R., Simaan, M.A., and Antaki, J. (1998). Estimation of systemic vascular bed parameters for artificial heart control. *IEEE Transactions on Automatic Control*, 43(6), 765–778.